Kann, B., Windbergs, M.
Chemical imaging of drug delivery systems with structured surfaces-a combined analytical approach of confocal raman microscopy and optical profilometry
(2013) AAPS Journal, 15 (2), pp. 505-510.

The AAPS Journal, Vol. 15, No. 2, April 2013, pp. 505-510
DOI: 10.1208/s12248-013-9457-7

Chemical imaging of drug delivery systems with structured surfaces – a combined analytical approach of confocal Raman microscopy and optical profilometry

Birthe Kann[1], Maike Windbergs[1,2,3,*]

[1]Department of Biopharmaceutics and Pharmaceutical Technology, Saarland University, Campus A4.1, 66123 Saarbruecken, Germany

[2]Helmholtz-Institute for Pharmaceutical Research Saarland, Campus C2.3, 66123 Saarbruecken, Germany

[3]PharmBioTec GmbH, Campus C2.2, 66123 Saarbruecken, Germany

*corresponding author:
Maike Windbergs
Department of Biopharmaceutics and Pharmaceutical Technology, Saarland University, Campus A4.1, 66123 Saarbruecken, Germany
Email: m.windbergs@mx.uni-saarland.de
Phone: +49 681 302 4763
Fax: +49 681 302 4677

Running head:
Confocal Raman microscopy and optical topography

Key words:
chemical imaging, drug delivery systems, confocal Raman microscopy, optical topography

ABSTRACT

Confocal Raman microscopy is an analytical technique with a steadily increasing impact in the field of pharmaceutics as the instrumental setup allows for non-destructive visualization of component distribution within drug delivery systems. Here, the attention is mainly focused on classic solid carrier systems like tablets, pellets or extrudates. Due to the opacity of these systems, Raman analysis is restricted either to exterior surfaces or cross sections. As Raman spectra are only recorded from one focal plane at a time, the sample is usually altered to create a smooth and even surface. However, this manipulation can lead to misinterpretation of the analytical results. Here, we present a trend-setting approach to overcome these analytical pitfalls with a combination of confocal Raman microscopy and optical profilometry. By acquiring a topography profile of the sample area of interest prior to Raman spectroscopy, the profile height information allowed to level the focal plane to the sample surface for each spectrum acquisition. We first demonstrated the basic principle of this complementary approach in a case study using a tilted silica wafer. In a second step, we successfully adapted the two techniques to investigate an extrudate and a lyophilisate as two exemplary solid drug carrier systems. Component distribution analysis with the novel analytical approach was neither hampered by the curvature of the cylindric extrudate nor the highly structured surface of the lyophilisate. Therefore, the combined analytical approach bears a great potential to be implemented in diversified fields of pharmaceutical sciences.

INTRODUCTION

Raman spectroscopy is a versatile technique for contactless and label-free characterization of diverse samples with a constantly growing impact in pharmaceutical sciences. It facilitates chemically selective analysis without sample destruction and can be used for component distribution analysis, discrimination between different molecular conformations and interaction studies. For pharmaceutical investigations, Raman spectroscopy with a sensor probe recording single Raman spectra is extensively used ranging from bulk material identification and counterfeit detection (1, 2) up to sophisticated applications such as PAT (process analytical technology) tools for process monitoring upon manufacturing (3, 4). To obtain spatially resolved, three-dimensional chemical information a Raman spectrometer can be implemented into a confocal microscope. The acquired spectral information is converted into chemically selective spatially resolved false color images. Confocal Raman microscopy is applicable for investigations of diverse drug delivery systems. In this context, the Raman mapping capabilities of the instrument have already been exploited to image the distribution of API (active pharmaceutical ingredient) and excipient(s) within a carrier system (5-7), API release (5-7) as well as interactions of small delivery systems with cells (8, 9).

As most customary samples in pharmaceutics feature gradual opacity, the analysis is often restricted to surface structures representing either the outer surface or cross sections. In any case the majority of these surfaces is structured. However, a confocal setup requires a smooth sample surface as the spectral information is collected from the focal plane. Therefore, different invasive methods of sample preparation such as polishing are often employed prior to Raman analysis to create a smooth sample surface. This can falsify the analytical results due to changes in the original composition i.e. luting and physical structure of the sample and should therefore be avoided. In pharmaceutics the impact of such analytical results is crucial as misleading data can affect further development procedures. It would be highly desirable to establish an analytical approach to combine confocal Raman microscopy with a technique for surface analysis allowing chemically selective investigation of highly structured sample surfaces in their original state.

Among the established techniques for analyzing surface structures are atomic force microscopy and electron microscopy (10, 11). However, these techniques exhibit several limitations. For electron microscopy measurements the sample has to be sputter coated prior to investigations, thus impeding further analysis with another technique such as Raman spectroscopy. Moreover, the techniques are usually restricted to the investigation of a small sample section, which is often not sufficient for the analysis of common solid carrier systems like extrudates, pellets or tablets. Atomic force microscopy can be combined with Raman spectroscopy, however, the technique is generally limited to sampling in submicrometer scale. Another microscopic approach is optical profilometry which has already been applied in manifold fields of applications ranging from ink to minerals (12-18). The technique is based on white light scattering after irradiating the sample of interest. The wavelength information of the detected scattered light represents the specific distance between light probe and sample surface which is converted into a topographic profile. Due to its non-destructive nature, optical profilometry suits as a complementary technique for confocal Raman microscopy.

In this study, we present the combined application of optical profilometry with confocal Raman microscopy for all-encompassing chemically selective analysis. In a first attempt, we proved the basic practicability of the combined approach by imaging a tilted silica wafer with a laser induced mark. In a second step, we adapted the approach for pharmaceutical purposes by analyzing two exemplary drug delivery systems. A cylindric extrudate consisting of a matrix former in which the drug has been embedded was investigated focusing on component distribution in the core and on the surface. Furthermore, a highly structured lyophilisate loaded with a protein in active and inactive state was analyzed detecting the localization of inactive drug.

MATERIALS AND METHODS

Sample preparation

Extrudate: A powder mixture consisting of 50% (w/w) tripalmitin (Sasol, Witten, Germany) and 50% (w/w) theophylline anhydrate (BASF, Ludwigshafen, Germany) was fed into a co-rotating twin-

screw extruder (Mikro 27GL-28D, Leistritz, Nuernberg, Germany) with a feeding rate of 40 $gmin^{-1}$. The mass was extruded through a die plate with 23 holes (diameter 1 mm, length 2.5 mm) with a screw speed of 30 rpm and a processing temperature of 55 °C.
Lyophilisate: Bovine Serum Albumin (BSA) was purchased from Sigma Aldrich. Thermally denaturated protein was prepared by heating the protein dissolved in water for 90 min at 100 °C and verifying the conformation by Raman microscopy. An aqueous solution containing a mixture of native and thermally denaturated BSA was freeze dried in a freeze dryer alpha 2-4 LSC (Christ, Osterode, Germany) for 48 hours with a final drying step for 1 hour.

Scanning electron microscopy (SEM)
Samples were sputter coated with gold. SEM measurements were performed by a Zeiss EVO HD15 electron microscope at an accelerating voltage in a range of 3 to 5 kV.

Optical profilometry
True surface microscopy was performed with a WITec alpha 500/300T+ (WITec GmbH, Ulm, Germany). No sample preparation was needed. The sensor probe can resolve an elevation difference of 3 mm with a step size of 120 nm along the z-axis. A silica wafer section of 150 µm x 100 µm and a pixel size of 2 µm x 2 µm was irradiated with an integration time of 0.1 sec. The exterior extrudate surface was rasterized at a step size of 5 µm along the x and y axes with an integration time of 0.1 sec. The lyophilisate area under investigation was 2000 µm x 2000 µm. Every 50 µm in both x and y direction a signal was recorded with an integration time of 0.05 sec.

Raman spectroscopy
Raman spectra were recorded with a confocal Raman microscope WITec alpha 500/300R+ (WITec GmbH, Ulm, Germany) using implemented Zeiss objectives (50 x NA = 0.55; 50 x NA = 0.8; 10 x NA = 0.25). The excitation wavelength of the Nd:YAG laser was 532 nm actuated at 10 mW (lyophilisate), 30 mW (extrudate) or 40 mW (silica wafer). Signals were detected by a back-illuminated CCD camera after passing a 50 µm pinhole. The spectral resolution was 4 cm^{-1}. The wafer image had a pixel resolution of 2 µm x 2 µm. Integration time for each Raman spectrum acquisition was 0.2 sec. Raman spectra were recorded every 5 µm x 5 µm along the x and y axis for the extrudate cross section and exterior surface integrated at 0.1 sec and 0.5 sec, respectively. 2500 Raman spectra were collected from the investigated lyophilisate area of 2000 µm x 2000 µm at an integration time of 0.6 sec. No preparation was performed for any sample prior to investigation. The collected Raman spectra were processed and converted into false color images using the software WITec Project Plus (WITec GmbH, Ulm, Germany).

RESULTS AND DISCUSSION

To prove the practicability of the analytical approach combining confocal Raman microscopy with optical topography and to elucidate its potential, we first investigated a silica wafer with a laser induced mark as a well defined sample. The wafer itself exhibited a smooth surface and silica is a strong Raman scatterer facilitating the acquisition of Raman spectra. For the proof of concept experiment, we tilted the wafer creating an inclined plane. These surface conditions impaired a comprehensive characterization with a conventional confocal Raman microscope as spectra acquisition was limited to one focal plane at a time (Fig. 1a). Therefore, the analysis of the wafer surface without individual manual focusing for each spectrum was rendered impossible.

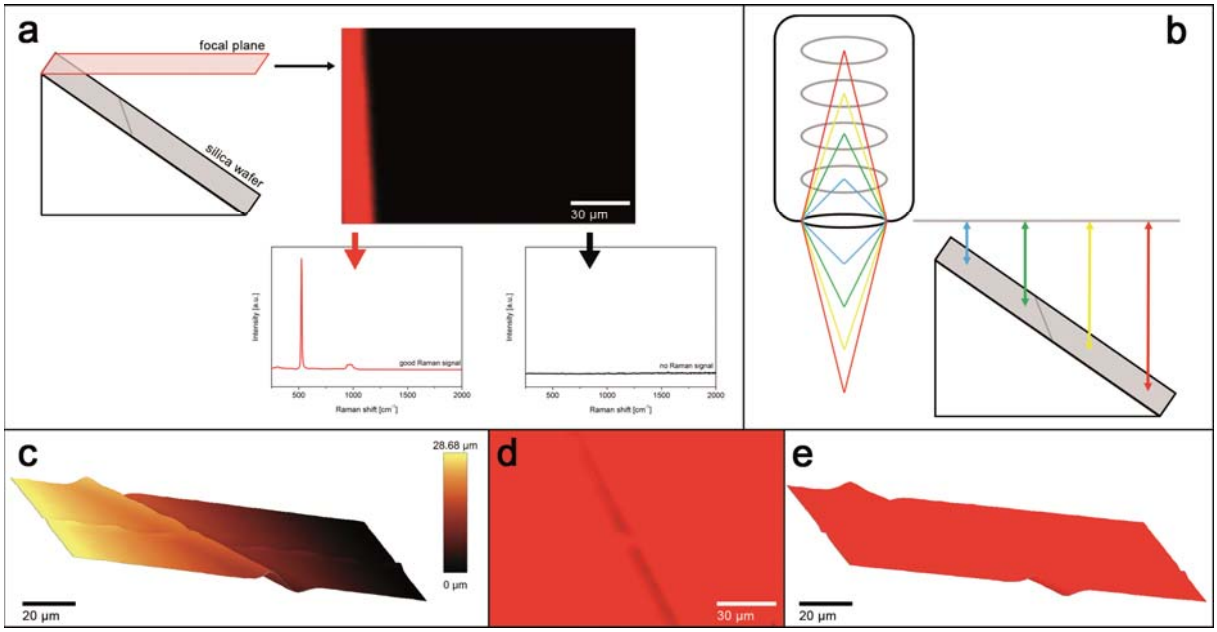

Figure 1. Combination of Raman microscopy and optical profilometry as complementary analytical techniques. a) Raman spectra acquisition of a tilted surface with a conventional microscope was limited to the focal plane (visible by the red area in the microscopic image). b) Schematic principle of optical profilometry. White light is focused on the sample surface and according to the distance between probe and surface the respective wavelength of the white light is selectively collected by the detector. c) Surface topography profile of a tilted silica wafer. d) Two dimensional false color Raman image of the same tilted silica wafer area. e) Overlay of topography profile and confocal Raman microscopy analysis data resulting in a three dimensional chemically selective false color image.

Optical topography is based on a white light source and an optical probe. The probe contains a hyperchromatic lens assembly having a distinct linear chromatic error. As white light is composed of different colors (different wavelengths), each color has a unique focal distance. By focusing the light onto the sample and collecting the backscattered light through a pinhole, only the color in focus can be detected according to the distance between the probe and the sample surface (Fig. 1b). This information is subsequently converted into topographic height differences. A wafer section of 150 µm x 100 µm was first investigated with the profilometry probe to create the topographic map of the area of interest (Fig. 1c). The subsequent recording of the Raman spectra from the same area was guided by the profilometry information, thus the microscope focus was individually adjusted according to the sample topography while the sample surface was rasterized for Raman spectra acquisition. Therefore, at every measurement point the focal plane was positioned at the sample surface which is the key to obtain all-encompassing chemically selective characterization. For component distribution analysis, a confocal microscope is a compulsory feature as confocality is a prerequisite for the mapping capability. The recorded Raman spectral data set was converted into a false color image, where each component is represented by a different color. The false color image is a two dimensional depiction (Fig. 1d). However, when overlaying the topography profile with the two dimensional Raman image in a subsequent step, a three dimensional spatially resolved image was obtained (Fig. 1e).

After this initial proof of concept study, we applied the complementary analytical approach on two different drug delivery systems to evaluate the suitability of the combined techniques for pharmaceutical purposes. In a first step, we investigated lipid-based extrudates, a solid oral dosage form exhibiting a cylindric morphology. These drug delivery systems were obtained after extrusion of physical powder mixtures and have already been thoroughly characterized in the past (19-21). However, analysis of component distribution with confocal Raman microscopy has thus far been limited to cross sections as the curvature of the cylindric form impaired analysis of the exterior surface. Nevertheless, the interior component ratio does not automatically represent the exterior distribution of the components due to the manufacturing procedure. In pharmaceutical production extrudates are often intermediate products mainly processed into pellets. Therefore, a thorough understanding of the

initial solid dosage form is of vital importance to evaluate subsequent steps like spheronization. Here, we analyzed extrudates composed of the lipid matrix former tripalmitin and theophylline anhydrate as API regarding their interior and exterior component distribution. As extrudates are opaque systems, the sample was manually cut with a razor blade creating an artificial surface prior to Raman investigations. The light microscopy image in Figure 2a shows the created smooth surface which was suited for immediate confocal Raman microscopy investigation without further sample preparation. The recorded Raman spectra of the cross section were subsequently converted into false color images. The false color Raman image showing the homogeneous distribution of both components within the created cross sections is visualized in Figure 2a. For better demonstration of the instrument's mapping capabilities, the individual false color images with the respective Raman spectra of each component tripalmitin and theophylline anhydrate are depicted in Figure 2b.

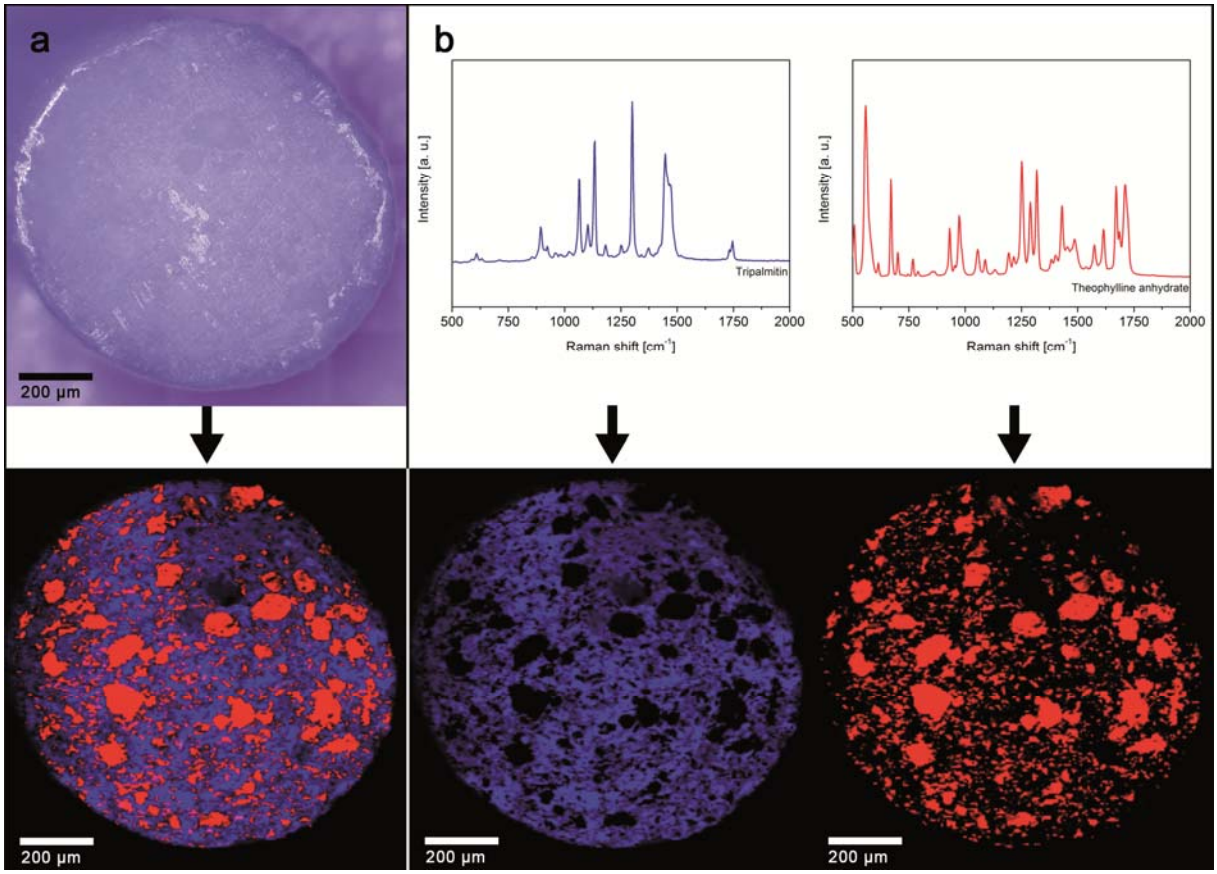

Figure 2. Component distribution analysis of the interior ratio of an extrudate. a) Light microscopy image of the investigated extrudate cross section and the resulting false color Raman image. Tripalmitin is represented in blue, whereas theophylline anhydrate is indicated in red. b) Raman spectra of each component and the respective individual false color Raman images of the two components tripalmitin (blue) and theophylline anhydrate (red).

Raman mapping of the extrudate cross section is a well suited technique to portray the component distribution. However, as mentioned before, the interior component distribution does not automatically equal the exterior ratio. Therefore, it would be eligible to use mapping as well to visualize the exterior component ratio. The exterior extrudate surface is smooth but exhibits a curvature (Fig. 3a), thus impeding analysis with a conventional confocal Raman microscope. If initially acquiring a topography profile of the curved surface, Raman mapping can be performed in a subsequent step. Figure 3b shows a topography profile of an extrudate section. The symmetric gradient of the color scale nicely demonstrates the curvature and therefore, the precise functioning of the optical sensor probe. The subsequently derived Raman spectral data set was recorded by rasterizing the surface where the topography background information guided the focal point along the curvature of the extrudate. The single Raman spectra for each component are shown in Figure 3c. To visualize the exterior

component ratio, the spectral data set was converted into a chemically selective false color Raman image. By overlaying the topography profile with the Raman image, we obtained not only a chemically selective but also spatially resolved image in three dimensions. Therefore, the analytical results of the extrudate could be examined from different angles (Fig. 3d). In this exemplary case study, the component distribution was homogenous for the cross section image as well as for the topography corrected surface image. Thus, the exterior component ratio did reflect the interior distribution of the extrudate.

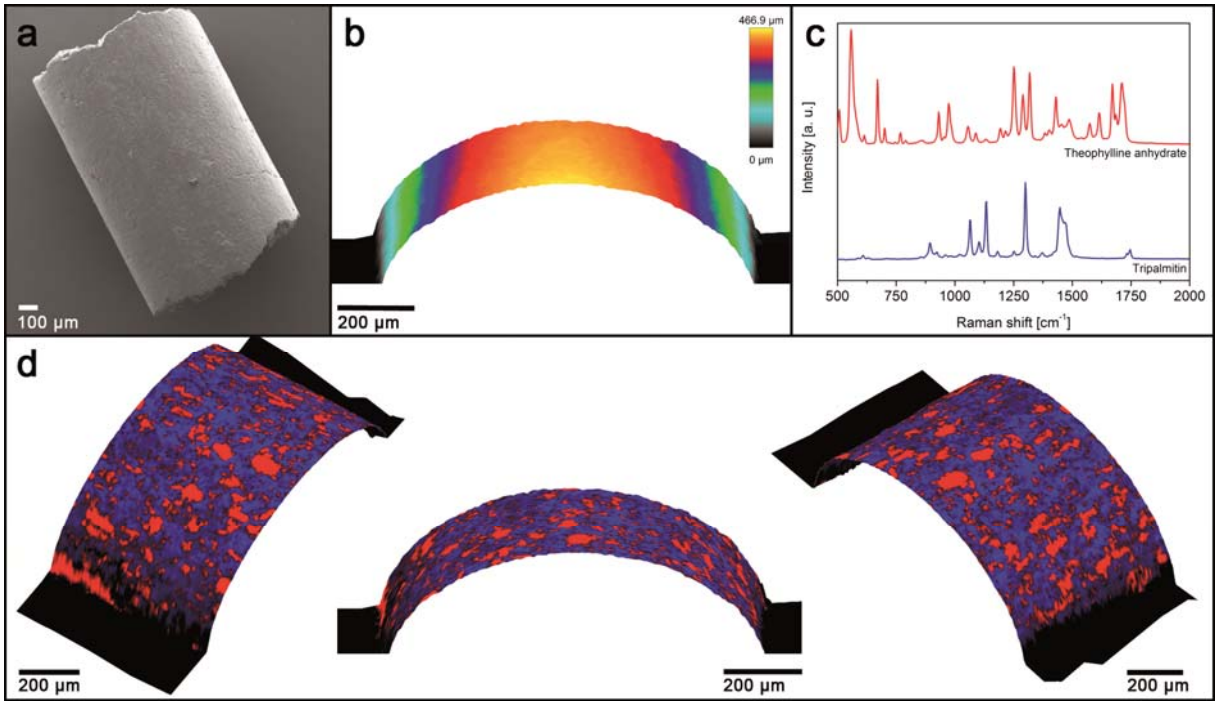

Figure 3. Component distribution analysis of the exterior extrudate surface. a) Electron microscopy image of an extrudate. b) Topography profile of the extrudate showing the curvature of the exterior surface. c) Single Raman spectra of the individual components tripalmitin (blue) and theophylline anhydrate (red). d) Overlay of topography profile with false color Raman image from different angles depicting component distribution on the exterior surface. Tripalmitin is shown in blue and theophylline anhydrate in red.

As a second example, we fabricated a lyophilisate containing the protein drug BSA in its native and denaturated conformation. The lyophilisate formed a white solid cake-like structure with opaque optical properties (22). In contrast to the extrudate which we investigated first, the lyophilisate exhibited a rough and highly structured surface (Fig. 4a). The detailed structure was visualized by electron microscopy in Figure 4a.

Analytical detection of the protein structural change with Raman microscopy was performed by using the so called amide I band at 1500 - 1800 cm^{-1} (22-26). The amide I band is generally used to detect changes in the secondary structure of proteins. The Raman signal of this band is mainly derived from the C=O vibrations of the amide groups in the peptide backbone (23, 26). A shift of this band in the Raman spectrum is a clear indication for conformational changes (25, 26). Thus, the technique is capable to discriminate between therapeutically active and inactive protein structure within the lyophilisate. The embedded BSA in its native and denaturated form can be distinguished by its respective Raman spectra as highlighted in Figure 4b.

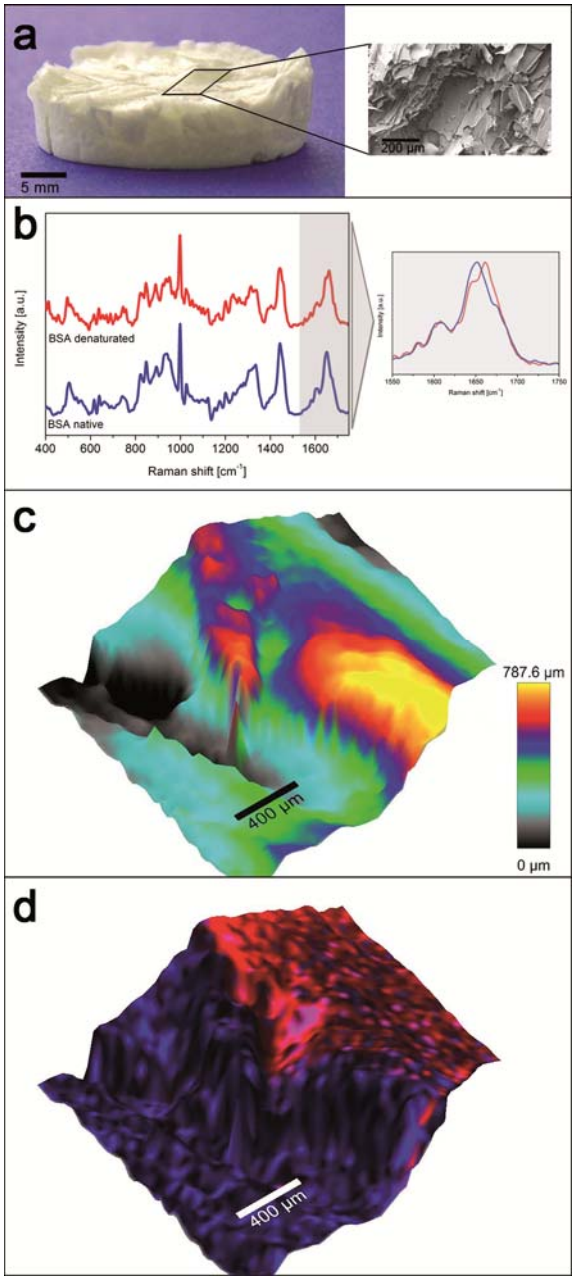

Figure 4. Investigation of a highly structured lyophilisate section regarding protein conformation location. a) Lyophilisate and electron microscopy image of an enlarged area visualizing the highly structured surface. b) Raman spectrum of BSA in its native (blue) and denaturated (red) conformation. The shift of the Amide I band between the two conformations is highlighted. c) Surface topography profile of a lyophilisate section. d) Overlay of topography profile and respective Raman microscopy analysis data. The resulting three dimensional chemically selective false color image indicates the native protein in blue, whereas red represents the denaturated protein conformation.

Therefore, we created a sample challenging the abilities of the analytical setup. Unlike wafer and extrudate, which showed different morphologies but still exhibited a smooth plane, the lyophilisate had an irregular, fragile surface structure. Furthermore, the component discrimination was mainly based on a marginal spectral difference of one specific peak shift for the lyophilisate, whereas the aforementioned samples were composed of different chemical components showing completely different Raman spectra. In any case, for a versatile application in pharmaceutics the combined analytical approach of confocal Raman microscopy and optical topography should cope with diverse sample specifications.

Following the analytical order of performing optical topography prior to confocal Raman microscopy analysis, a topography profile of a lyophilisate section of 2000 µm x 2000 µm was created as shown in Figure 4c. The subsequently recorded Raman spectra were then converted into false color images, indicating each BSA conformation in a different color. The native conformation of BSA is represented in blue whereas the denaturated conformation is shown in red. In a final step, an overlay of the topographic profile with the Raman image was created by merging the two individual maps (Fig. 4d). For both techniques, the same area with the identical grid for collection of scattered light was rasterized. Thus, the individual maps were composed of analytical information derived from exactly the same sample spot, enabling the overlay of these complementary data with utmost precision. Ultimately, a three dimensional characterization of the sample was obtained combining chemical selectivity and surface properties in a spatially resolved image.

CONCLUSION

We successfully introduce the combined analytical approach of confocal Raman microscopy and optical profilometry for investigation of structured surfaces in pharmaceutical science. After proving the concept of the approach, two different drug delivery systems were successfully analyzed regarding their component distribution. The extrudate was built of two components and exhibited a curved surface whereas the challenge for the lyophilisate analysis was based on an unpredictable surface structure and only consisted of one component in two different conformations. Although components and exhibited surface structures varied broadly, precise images regarding spatial resolution and chemical selectivity were obtained. Therefore, the analytical technique is valid for a wide use in pharmaceutical research. The advantage of the non-destructive principle and the informative detailed result outcome bears a high potential for the extensive use of the complementary techniques confocal Raman microscopy and optical profilometry for pharmaceutical investigations.

ACKNOWLEDGEMENTS

The authors thank Thomas Dieing for support and valuable discussions.

REFERENCES

(1) Been F, Roggo Y, Degardin K, Esseiva P, Margot P. Profiling of counterfeit medicines by vibrational spectroscopy. Forensic Sci Int. 2011;211:83–100.
(2) de Veij M, Deneckerea A, Vandenabeele P, de Kaste D, Moens L. Detection of counterfeit Viagra® with Raman spectroscopy. J Pharm Biomed Anal. 2008;46:303–309.
(3) Wirges M, Mueller J, Kása Jr. P, Regdon Jr. G, Pintye-Hódi K, Knop K, Kleinebudde P. From mini to micro scale-feasibility of Raman spectroscopy as a Process Analytical Tool (PAT). Pharmaceutics. 2011;3:723-730.
(4) De Waard H, de Beer T, Hinrichs WLJ, Vervaet C, Remon JP, Frijlink HW. Controlled crystallization of the lipophilic drug fenofibrate during freeze-drying: Elucidation of the mechanism by in-line Raman spectroscopy. AAPS J. 2012;12:569-575. doi: 10.1208/s12248-010-9215-z.
(5) Windbergs M, Haaser M, McGoverin C, Gordon K, Kleinebudde P, Strachan CJ. Investigating the relationship between drug distribution in solid lipid matrices and dissolution behavior using Raman spectroscopy and mapping. J Pharm Sci. 2010;99:1464-1475.
(6) Haaser M, Windbergs M, McGoverin CM, Kleinebudde P, Rades T, Gordon KC, Strachan CJ. Analysis of matrix dosage forms during dissolution testing using Raman microscopy. J Pharm Sci. 2011;10:4452-4459.
(7) Belu A, Mahoney C, Wormuth K. Chemical imaging of drug eluting coatings: combining surface analysisi and confocal Raman microscopy. J Control Release. 2008;126:111-121.
(8) Matthaeus C, Kale A, Chernenko T, Torchilin V, Diem M. New ways of imaging uptake and intracellular fate of liposomal drug carrier systems inside individual cells, based on Raman microscopy. Mol Pharmaceut. 2008;5:287-293.

(9) Chernenko T, Matthaeus C, Milane L, Quintero L, Amiji M, Diem M. Label-free Raman spectral imaging of intracellular delivery and degradation of polymeric nanoparticle systems. ACS Nano. 2009;3:3552-3559.
(10) Sheparovych R, Motornov M, Minko S. Low adhesive surface that adapt to changing environments. Adv Mater. 2009;21:1840-1844.
(11) Schrank S, Hodzic A, Zimmer A, Glasser BJ, Khinast J, Roblegg E. Ibuprofen-loaded calcium stearate pellets: Drying-induced variations in dosage form properties. AAPS Pharm Sci Tech. 2012;13:686-698.
(12) López AJ, Rivas T, Lamas J, Ramil A, Yáñez A. Optimisation of laser removal of biological crusts in granites. Appl Phys A: Mater Sci Process. 2010;100:733-739.
(13) Truong VK, Lapovok R, Estrin YS, Rundell S, Wang JY, Fluke CJ, et al. The influence of nano-scale surface roughness on bacterial adhesion to ultrafine-grained titanium. Biomaterials. 2010;31:3674-3683.
(14) Azmat NS, Ralston KD, Muster TH, Muddle BC, Colel S. A high-throughput test methodology for atmospheric corrosion studies. Electrochem Solid-State Lett. 2011;14:C9-C11.
(15) Feys J, Vermeir P, Lommens P, Hopkins SC, Granados X, Glowacki BA, et al. Ink-jet printing of $YBa_2Cu_3O_7$ superconducting coatings and patterns from aqueous solutions. J Mater Chem. 2012;22:3717-3726.
(16) Schneider T, Kohl B, Sauter T, Becker T, Krantz K, Schossig M, et al. Viability, adhesion and differentiated phenotype of articular chondrocytes in degradable polymers and electro-spun structures thereof. Macromol Symp. 2011;309/310:28-39.
(17) Formosa LM, Mallia B, Bull T, Camelleri J. The microstructure and surface morphology of radiopaque tricalcium silicate cement exposed to different curing conditions. Dent Mater. 2012;28:584-595.
(18) Manova D, Lutz J, Maendl S. Sputtering effects during plasma immersion ion implantation of metals. Surf Coat Technol. 2010;204:2875-2880.
(19) Thommes M, Baert L, Rosier J. 800mg Darunavir tablets prepared by hot melt extrusion. Pharm Dev Technol. 2011;16:645-650.
(20) Gueres S, Siepmann F, Siepmann J, Kleinebudde P. Drug release from extruded solid lipid matrices: Theoretical predictions and independent experiments. Eur J Pharm Biopharm. 2012;80:122-129.
(21) Windbergs M, Gueres S, Strachan CJ, Kleinebudde P. Two-step solid lipid extrusion as a process to modify dissolution behavior. AAPS Pharm Sci Tech. 2012;11(1):2-8.
(22) Wang W. Lyophilisation and development of solid protein pharmaceuticals. Int J Pharm. 2000;203:1-60.
(23) Tantipolphan R, Rades T, Medlicott NJ. Insights into the structure of protein by vibrational spectroscopy. Curr Pharm Anal. 2008;4:53-68.
(24) Lippert JL, Tyminski D, Desmeules PJ. Determination of the secondary structure of proteins by laser Raman spectroscopy. J Am Chem Soc. 1976;98:7075-7080.
(25) Chen MC, Lord RC. Laser-excited Raman spectroscopy of biomolecules. VIII. Conformational study of bovine serum albumin. J Am Chem Soc. 1976;98:990-992.
(26) Hédoux A, Willart JF, Paccou L, Guinet Y, Affouard F, Lerbret A, Descamps M. Thermostabilization mechanism of BSA by trehalose. J Phys Chem B. 2009;113:6119-6126.